# A Treatment of Fission for HETC

**F. Atchison**
Paul Scherrer Institut
CH-5232 Villigen PSI
Switzerland

Abstract

The HETC code package allows modelling of complex nuclear facilities involving particles up to the few GeV energy region. In 1976, the package was implemented to support the engineering design of the target-moderator-reflector system for the ISIS pulsed spallation neutron source. The planned (and subsequently used) target material was uranium but the 'high-energy' part of the HETC package did not treat fission. A treatment of fission was built into the code and the current state of this is described.

# 1 Introduction

The current interest in accelerator-based transmutation of active waste and the relevance of fission to its study make it timely to describe in some detail the fission treatment in the version of the HETC[1] package used at PSI.

The engineering of components for use in and around regions bombarded by high-power density accelerator beams requires knowledge of heating rates, activation and damage rates. The components range in complexity from beam windows, secondary targets, beam dumps, etc. to 'spallation facilities' (e.g. neutron sources). The HETC code package (in its several versions) provides a basic Monte-Carlo nuclear physics 'tool-kit' to enable essential engineering design parameters to be calculated and also to carry out the nuclear design of the spallation facility itself.

A version of the HETC[2] package was obtained by the author from RSIC (*Radiation Shielding Information Centre, Oak Ridge National Laboratory*) in 1976 for use in supporting the engineering and neutronic design for the target-moderator-reflector system of the ISIS[3] pulsed neutron source. As uranium was to be the target material and the package in the form obtained did not allow for high-energy particle induced fission, a treatment had to be built in. That uranium was a good choice for the target material from the standpoint of neutronic performance was known from experimental studies[4]; the open questions were ones of detail and, principally, target dimensions' optimisation from the point of view of both neutronic performance and engineering of the neutron source.

The fission treatment has already been described[5] and was made available to the spallation neutron source community through the International Collaboration on Advanced Neutron Sources (ICANS): it is not known to the author which of the several versions of the HETC package have it built in or included as an option. Medium energy particle induced fission is likely to be significant in examining waste transmutation and users of versions of HETC with this fission treatment need to satisfy themselves that it is adequate. To assist in this process, a detailed description of the parameterisation is given here. Comparison of calculational results with experimental values carried out recently[6], led to some adjustment of parameter values.

# 2 The Treatment of Medium-Energy Particle Induced Fission

The emphasis is on fission induced by nucleons above about 15 MeV and pions above 2 MeV. In this energy region very little experimental information is available and reliance has to be put on theoretical estimates. Below this energy region, sufficient cross-section data exists. The essentials of the calculational model are similar to those of earlier studies by Dostrovsky et al.[7], Lindner & Turkevitch[8] and Hahn & Hermann[9]. The treatment invokes no new 'physics' and is applicable to light particles over a wide energy range: this has turned out to be useful for testing purposes.

## 2.1 Generalities

The essential physics of particle-nucleus interactions is handled in HETC by subroutine versions of the Bertini MECC code[10] and the evaporation code of Dresner[11] which together are a calculational realisation of the Serber[12] model. Apart from some minor changes (to be described below), these codes are accepted as the basis of the description of the interaction. In particular, it should be noted that pre-equilibrium emission is not included in the modelling of the particle-nucleus interaction.

Fission is a collective nuclear effect and takes place on a timescale that is long compared to the medium-energy intranuclear cascade; that is, fission will only be significant as a channel in competition with nucleon cluster evaporation. The end state of a nucleus after the intranuclear cascade can have high excitation energy (100 or more MeV) and proton & neutron numbers significantly below that of the struck nucleus. The end state for any one incident-particle + energy + struck-nucleus system is also highly variable. The subsequent evaporation process also can involve the ejection of several 10's of nucleons. That is, any treatment of the fission process as a competitor to evaporation has to be wide

ranging in Z, A and E*.

The version of the Dresner code incorporated into HETC uses a somewhat reduced statistical model treatment. In particular (i) nuclear spin is not considered, (ii) gamma emission is not treated as a competitive process, (iii) a slowly varying level density parameter of $\frac{A}{14}$ at low to $\frac{A}{13}$ at high mass is used and (iv) evaporation is restricted to neutrons, protons, deuterons, tritons, $^3He$-nuclei and $\alpha$-particles.

## 2.2 The Calculational Model for Fission

The logical flow of the overall particle-nucleus interaction with fission is shown in Fig. 1 and is the basis of the present calculational model. To calculate with it, two things have to be decided:

(i) the fission probability: writing $\Gamma_e$ and $\Gamma_f$ for the widths for evaporation and fission at some point in the de-excitation cycle, then the fission probability ($P_f$) is given by:-

$$P_f = \frac{\Gamma_f}{\Gamma_f + \Gamma_e} \tag{1}$$

(ii) the post-scission fragment nuclear state: charge, mass and excitation & recoil energies $\langle Z, A, E^*, T_{rec} \rangle$.

In making the parameterisation, the wide range of nuclear states for potential fissioning nuclei has to be kept in mind.

**General Assumptions**

The following general assumptions are made about the fission process:-

(i) The fission width depends only on the state of the nucleus and not on how it arrived there. The agreement between results of studies with a variety of projectiles to reach similar fissioning system states e.g. refs. 13, 14, supports this for the light projectiles transported in HETC. As part of the testing, the calculational model has also been applied to $\alpha$-particle induced fission.

(ii) Fission competes at all stages of nuclear de-excitation.

(iii) Only binary fission will occur. In terms of the calculational flow (see Fig. 1), this means that fission is locked-off for the fission fragments.

(iv) The mass split is always complete. The two fragments will conserve baryons and charge. This means that, for example, the 'fission' neutrons will come from either evaporation prior to fission or from the fission fragments. Bowman et al.[15] found that 90% of the neutrons from the spontaneous fission of $^{252}Cf$ came from the fully accelerated fragments.

(v) Fission for nuclei with Z less than 70 is not considered. Apart from not wasting computer time on insignificant contributions, this avoids restricting global correlations to yielding 'sensible' values over the complete range of nuclei.

**Fission Probability:**

The treatment has been split between the elements above and below Z = 89. There are two reasons: (i) there is very little experimental information on fission in the region Z = 85 to 88, (ii) the marked rise in the fission barrier for nuclei with $\frac{Z^2}{A}$ below about 34 (see Fig. 2) together with the disappearance of assymetric mass splitting, indicates that a change in the character of the fission process occurs. If experimental information were available, a split between regions about $\frac{Z^2}{A} \approx 34$ would more sensible.

Fission is only being considered for heavy nuclei for which evaporation is dominated by neutron emission. This means that the evaporation may be adequately represented by the width for neutron emission, $\Gamma_n$.

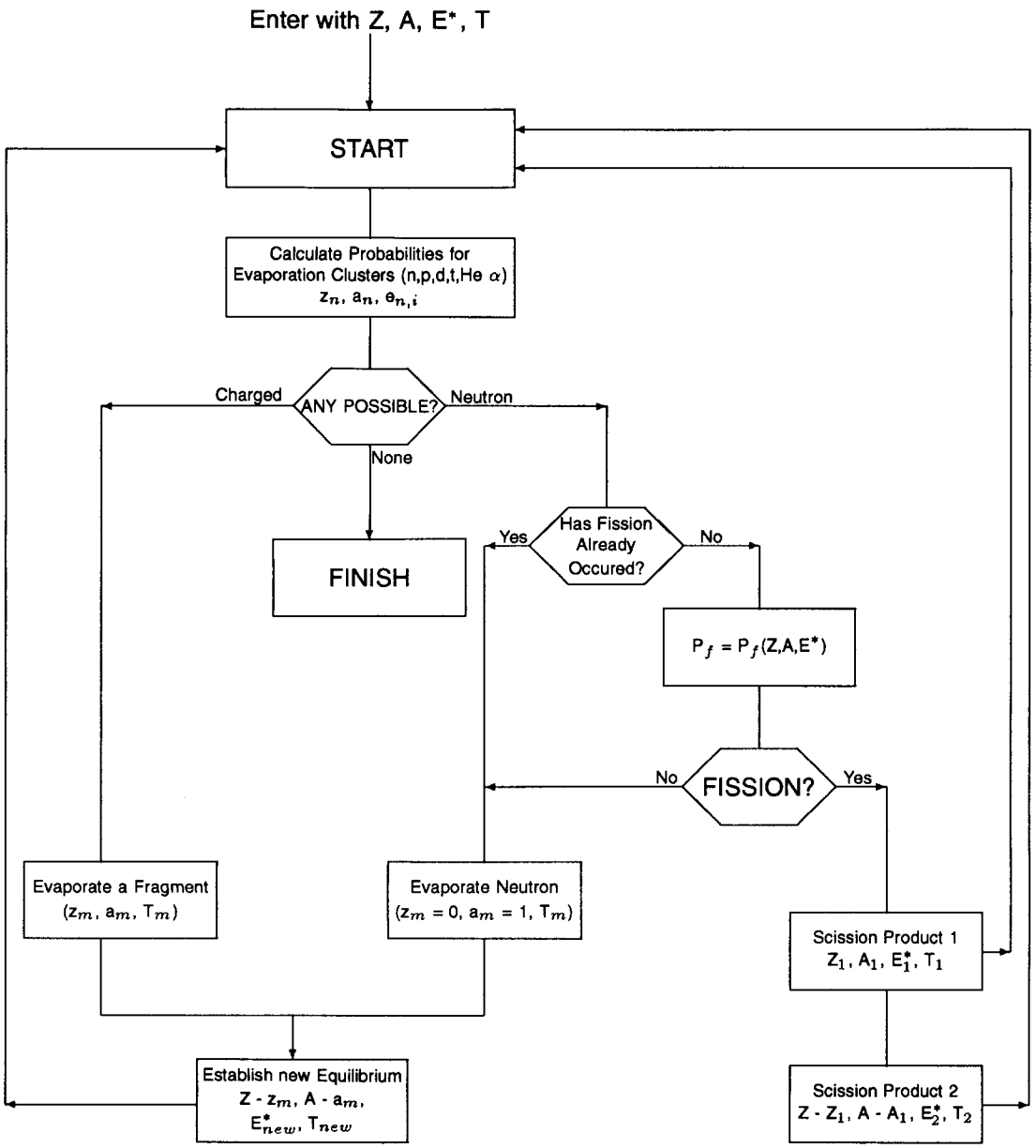


Figure 1: **The logical flow for evaporation including fission.**

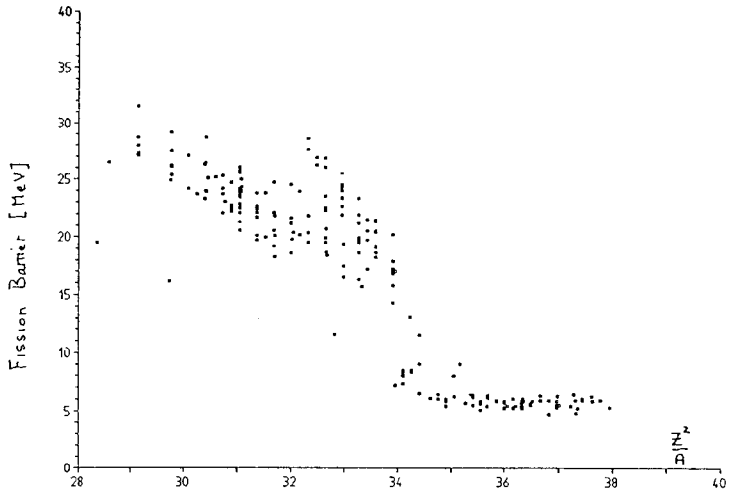


Figure 2: **Measured fission barriers as a function of $Z^2/A$. The data comes from Dahlinger et al.[16]**

**Table-I**

**Present Values for the Constants in Equation 2.**

| Z | 89 | 90 | 91 | 92 | 93 | 94 | 95 | 96 | 97 | 98 | 99 | 100 |
|---|---|---|---|---|---|---|---|---|---|---|---|---|
| $A_0(Z)$ | 221.6 | 225.8 | 230.1 | 234.4 | 238.63 | 241.34 | 243.04 | 245.52 | 246.84 | 250.18 | 254.0 | 257.8 |
| $C(Z)$ | 0.154 | 0.175 | 0.169 | 0.165 | 0.165 | 0.15735 | 0.16597 | 0.17589 | 0.18018 | 0.19568 | 0.16313 | 0.17123 |

Both evaporation and fission are described in terms of the statistical model (Weisskopf[17], Bohr & Wheeler[18]) and fission experiments (e.g. Back et al.[19], Czyzewski et al.[20], Burnett et al.[21]) analysed with it to yield fission barriers.

For the high Z region, fission barriers are low and the expressions are complicated by the need to treat (double humped) barrier penetration, single particle effects and gamma emission competition and, as such, are unsuitable for use in Monte-Carlo. In the Z region above 88, the observation of Vandenbosch & Huizenga[13] that $\frac{\Gamma_n}{\Gamma_f}$ is closely independent of excitation energy above a few MeV is exploited; they also obtained a good correlation of the width ratio with fissioning nucleus mass (A) which may be quantified as follows

$$Log_{10}\left(\frac{\Gamma_n}{\Gamma_f}\right) = C(Z)\cdot(A - A_0(Z)) \tag{2}$$

where $C(Z)$ and $A_0(Z)$ are constants dependent on the nuclear charge (Z) only. The values of these constants presently used are given in Table-I (Note: some adjustment of values have been made since the first version[5])

A constant fission barrier height of 6 MeV is used, based mainly on the experimental results of Back et al.[19], Back et al.[22] and Gavron et al.[23]. Barrier penetration is not considered; that is, the fission probability is calculated only for excitation energies $\geq$ 6 MeV and is zero below.

In the region Z below 89 and down to a code minimum of 70, neutron emission and fission widths are calculated using the statistical model with an energy-independent pre-exponential factor for the level density and inverse-reaction cross-sections for neutrons as used for the Dresner code. For a nucleus with Z, A and excitation energy $E^*$:-

$$\frac{\Gamma_n}{\Gamma_f} = k\alpha A^{\frac{2}{3}}\frac{(\beta\mathcal{I}_0(a_n,S_n)+\mathcal{I}_1)}{\mathcal{I}_0(a_f,S_f)} \tag{3}$$

where $k = \frac{2gmr_0^2}{\hbar^2}$, $g$ a statistical factor (= 2 for neutrons), $m$ is the neutron mass and $r_0$ is the nuclear radius constant (taken to be 1.35 fm) and $\mathcal{I}_0$ and $\mathcal{I}_1$ are the statistical integrals given by:-

$$\begin{aligned}
\mathcal{I}_0(a,S) &= \frac{1}{2a}(1+(S-1)\exp^S) \\
\mathcal{I}_1 &= \frac{1}{8a_n^2}(S_n^2-6+(6-6S_n+2S_n^2)\exp^{S_n}) \\
&\quad where \\
S_n &= 2\sqrt{a_n(E^*-E_n)} \\
a_n &= \frac{1}{8}(A-1) \\
S_f &= 2\sqrt{a_f(E^*-E_f)}
\end{aligned}$$

$a_n$ and $a_f$ are the level density parameters for neutron emission and fission respectively, $E_n$ is the neutron separation energy, $E_f$ is the fission barrier height and $E^*$ is the excitation energy. The constants $\alpha$ and $\beta$ come from the inverse reaction cross-section parameterisation used by Dresner:

$$\begin{aligned}
\sigma(\varepsilon) &= \pi r_0^2 A^{\frac{2}{3}}\alpha(1+\frac{\beta}{\varepsilon}) \\
\alpha &= \frac{1.93}{A^{\frac{1}{3}}}+0.76 \\
\alpha\beta &= \frac{1.66}{A^{\frac{2}{3}}}-0.05
\end{aligned}$$

Values for the fission barrier, $E_f$, and the level density parameter for fission, $a_f$, have been obtained from a global parameterisation of fits, using $E_f$ and $a_f$ as variables, to measured values of $\frac{\Gamma_f}{\Gamma_n}$ from Huizenga et al.[24], Raisbeck & Cobble[25] and Burnett et al.[21]. The global parameterisations have been made in terms of $E_n$ (the neutron separation energy), $a_n$ the level density parameter for neutron emission ($a_n = \frac{A}{8}$ turned out to be more appropriate to obtaining a reasonable global fit than the value in the Dresner code) and $\frac{Z^2}{A}$ $(= \mathcal{X})$ and are:

$$E_f - E_n = 1.9624 + 0.2185(38.222-\mathcal{X})^2 \quad (4)$$

$$\frac{a_f}{a_n} = 1.0893 + 0.011(\mathcal{X}-31.086)^2 \quad (5)$$

In the evaluation of the equation for the fission barrier, the quadratic term is dropped should an $\mathcal{X}$ of greater than 38.222 occur!

The statistical model fits have been made with excitation energy independant level density parameters. As $a_f > a_n$, this leads to ever increasing values for $\frac{\Gamma_f}{\Gamma_n}$ and fission probabilities tending to 1 for all nuclei. That $a_f$ should tend to $a_n$ at high excitation energies comes out of calculations of level densities based on single particle schemes[26]. Statistical model fits including these show good agreement with measurement[26,27]. No satisfactory global prescription applicable to the case in hand could be found.

The most satisfactory prescription found so far is to reduce the fission probability by an approximate estimate for the number of chances; that is, for an average emission energy $Q_e$ (the sum of the Q value and the average kinetic energy) and an excitation energy $E^*$, the fission probability is computed from

$$P_f = \frac{C}{1+\frac{\Gamma_n}{\Gamma_f}} \quad where \quad C = min(1.0, \frac{Q_e}{E^*}) \quad (6)$$

The final problem to be solved was the severe suppression of charged particle emission particularly in the high Z region. This is caused by the bias of evaporation to emission of neutrons plus the increase

of fissionability as the mass (at a given Z) is reduced. Following investigations of both fission cross-sections and spallation product mass distribution in comparison with available data under a variety of prescriptions, the following two changes were adopted:-

- To introduce an excitation energy dependent coulomb barrier in accordance with the prescription of Le Couteur[28] to help evaporation of charged particles at higher excitation energies.
- To restrict fission competition to neutron emission only (see Fig. 1). That is, when the evaporation sampling algorithm selects charged particle emission, by-pass fission competition.

## 2.3 Post-Scission Parameter Selection

The choice of charge, mass, excitation energy and recoil kinetic energy for the two fission fragments is based on available systematics. Their choice will affect the subsequent neutron yield and the final nuclide distribution. The ordering of the following roughly reflects the increasing difficulty of finding clear guidance in making parameter selection.

**Recoil Kinetic Energy**: Fission occurs as a roughly adiabatic process leading to no significant imparting of kinetic energy during passage over the saddle point. The kinetic energy is obtained from the coulomb repulsion between the two fragments when the scission is complete. A clear correlation between the sum kinetic energy of the two fragments ($E_{tot}$) and the coulomb parameter $\frac{Z^2}{A^{\frac{1}{3}}}$ (Vandenbosch & Huizenga[29], Unik et al.[30] , Hyde[31]) leads to the adoption of:

$$E_{tot} = 0.1065 \left( \frac{Z_1 Z_2}{A_1^{\frac{1}{3}} + A_2^{\frac{1}{3}}} \right) + 20.1 \tag{7}$$

Experimental data[29,30,32,33,34] suggests that the distribution is gaussian with a FWHM width of 15%.

The picking of the recoil energy follows after the split has been selected ($Z_1$, $A_1$, $Z_2$ and $A_2$) and is partitioned using energy and momentum conservation in the C.M. system.

**Charges**: Of the two possibilities, equal charge density or equal displacement from stability, there would seem to be no clear advantage for either. The picking is made after selection of the masses and based on equal distance from stability. The most stable charge number for a nucleus of mass A, $Z_s$, is given approximately by:-

$$Z_s(A) = \frac{A}{2 + 0.0156 A^{\frac{2}{3}}}$$

Then one charge is selected on the basis

$$Z_1 = Z_s(A_1) + \frac{1}{2}(Z - Z_s(A_1) - Z_s(A_2)) \tag{8}$$

and smeared with a gaussian of width 2 charge units. The other charge follows from conservation of Z.

**Mass**: For fission in the high Z region, the mass distribution for low excitation energy starts by being asymmetric with one mass at about 140 independent of the fissioning nucleus mass. As the excitation energy of the fissioning nucleus rises, an increasing contribution from symmetric mass splitting is observed. In the lower Z fissioning systems the mass split always seems centered about the half mass. An empirical relationship for the relative proportions of symmetric and asymmetric fission at a given excitation energy, $E^*$, suggested by experimental data is used:-

$$\frac{\Gamma_f^{Symm}}{\Gamma_f^{Asym}} = 2.05 \cdot 10^{-4} \exp^{0.36 E^*} \tag{9}$$

For asymmetric fission, the mass of the heavy fragment is picked from a gaussian of variance 6.5 mass units centered on a mass of 140.

For symmetric fission, a mass split about $\frac{1}{2}A$ is used with a gaussian spread of variance dependant on excitation energy above the fission barrier (Neuzil & Fairhall[35]):-

$$\sigma_{symm} = 0.425(0.935 + (E^* - E_f)(1 - 0.05(E^* - E_f))) \quad (10)$$

For consistency, the fission barrier values for $Z > 88$ and/or $\frac{Z^2}{A} > 35$ are taken from Seaborg & Vandenbosch[36]:-

$$E_f = 18.1 - 0.36\frac{Z^2}{A} + \epsilon \quad (11)$$

and where $\epsilon = 0.7$ for odd-odd nuclei, 0.4 for even-even nuclei and zero otherwise.

Outside this region, the values for $E_f$ come from the global systematic of equation 4. The picking procedure is protected to give a minimum mass of 5 for either fragment. The mass of one fragment only is picked (that of the higher in the case of asymmetric fission) and the other comes by conservation of A.

**Excitation Energy**: The excitation energy is based on distributing the excess of the binding energy release over the recoil kinetic energy (i.e. conserving energy over the scission process) on an equal density per nucleon basis; i.e. $\frac{A_1}{A_1+A_2}$ to fragment of mass $A_1$ etc.

If the excitation energy is predicted to be negative, the whole picking procedure is repeated: this is the only check that the selected split is physically reasonable.

### 2.4 Other HET Changes

Two modifications to a test version of the MECC/DRES codes have been introduced:-

- The upper mass limit of MECC in the original HETC is 239. The control subroutine of the MECC code (BERT) has been modified to allow masses up to 269 to be treated. Data for the nuclear density distribution (average radii, densities and well depths) have been derived by extrapolation of the high mass fixed data.
- Q-values are based on mass data from the 1983 evaluation of Wapstra & Audi[37] in place of the original data for DRES (based on the 1966 evaluation Mattauch et al.[38]) which only extended to a mass of 250. Data is stored in a library for $\pm 10$ charges about the most stable Z for a given A. Extrapolation to fill out missing values is based on a local fit to the form of the Cameron[39] mass formula. As for the original version of DRES, Q-values for nuclei outside the tabulated masses are derived from the Cameron mass formula.

## 3 Comparison of Calculated Values with Measurement

The treatment of fission seems to have been adequate for its original goal, as the ISIS system seems to perform[40,41] much as predicted[42]. Further evidence for reasonable agreement with experiment comes from measured fertile-to-fissile conversion and fission rates in thick targets of depleted uranium and thorium by 800 MeV protons made at Los Alamos[43].

The comparisons above are for large scale systems where many aspects of the full material cascade contribute, giving opportunity for error compensation.

### 3.1 Cross-sections for Fissionable Nuclei

A selection of cross-sections calculated with the evaporation code as modified to include fission have already been presented in reference 6 and only one or two that illustrate specific points will be included in this paper (references to the original figures will be given as FA92/Fig-X). The majority of the estimates come from Monte-Carlo with the number of events limited to reduce statistical error to below about 10%.

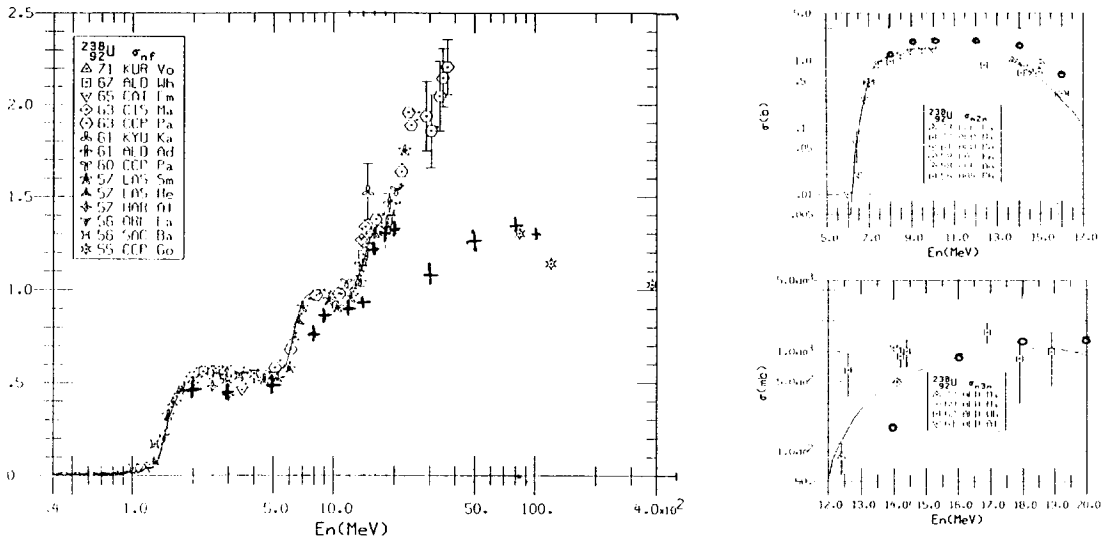


Figure 3: **Fast neutron cross sections for $^{238}U$. The calculated cross-sections are shown on curves taken from BNL-325.**

Comparison of fission cross-sections only are inadequate; in particular, all channels are relevant for activation estimates. The main goal is to treat fission in the energy range above about 15 MeV, which implies high excitation energies for the nuclei.

Fission of nuclei with high excitation energies have been studied experimentally mainly with ions. To allow these measurements to be included in the checking of the model, a locally written code for calculating light-ion interaction cross-sections using the Thomas[44] method has been used in combination with the fission-evaporation code. Potential function parameters are taken from Igo[45] for $\alpha$-particles. The $\alpha$-particle induced fission cross-sections used as the basis for the parameterisation of the statistical model as re-calculated may be seen in in FA92/Fig 19.

Further $\alpha$-particle cross-sections for heavy elements may be seen in FA92/Fig 20 for fission and spallation of $^{238}U$ [46,47,48] and $^{238}Pu$ [49] and a selection of ($\alpha$, 4n) cross-sections[51,50,52] in FA92/Fig 21. The agreement in the case of $^{238}U$ ($^{242}Pu$ as primary excited nucleus) is quite reasonable although the downward trend of the calculated spallation cross-section hints at overestimate for the fission probability for the lighter Pu isotopes. In the case of $^{242}Cm$ as primary excited nucleus, the calculation underestimates the spallation cross-section by more than an order of magnitude (but it should be noted that the spallation cross-section is less than 4% of that for fission). The ($\alpha$, 4n) cross-sections give a strong indication that the combined evaporation-fission treatment is modelling the measured process.

Some neutron induced cross-sections (mainly fission), calculated using the compound nucleus model with total cross-sections taken from ENDF/B-IV in the energy range up to 20 MeV and with MECC above, were given in FA92/Figs 22 to 25. These basically show the quality of the Vandenbosch & Huizenga[13] correlation but also that the evaporation treatment at low excitation energies is quite reasonable. In general the agreement is considered reasonable although for very high Z there is a strong indication that the parameterisation is not as good as at lower values: this might be expected due to the restricted amount of data available. The results for $^{238}U$ (shown in Fig. 3) highlight the inadequacy of the overall particle-nucleus treatment for the energy region where the transition from full compound-nucleus to full Serber model takes place.

Reasonable agreement with experimental results for medium-energy proton induced fission cross-sections[55,56,57,58] is also obtained (see FA92/Fig 26).

### 3.2 Mass Distribution

As medium-energy fission is a combination of contributions from several fissioning nuclei, both the fission and spallation product yields are relevant. Measurements of both fission and spallation products for the same particle-nucleus system have been found only for $^{238}U$ bombarded by 340 MeV protons: some of the fission products were measured by Stevenson et al.[53] and some spallation products by Lindner & Osborn[54]. The calculated and measured results are shown in Fig. 4. The two experiments disagree on the total fission cross-section, 1590 mb from Stevenson et al. and 1370 mb from Lindner & Osborn. The calculation gives 1330 mb.

The width for the fission products mass distribution is a little higher than the measured values (the calculated cross-sections at the peak are about 40% lower) and comparisons for spot nuclides are up to a factor of 10 lower.

Quite good agreement for the high-mass end of the spallation products is obtained and spot-nuclide cross-section values are within a factor of 2 to 4. For the total production rate of the heavy elements the agreement is also quite good (Np, 0.4 for measured over calculated; U, 1.1; Pa, 1.3; Th, 2.1; Ac, 1.2). The sum production cross-section for the mass 210 nuclides At, Po, and Bi was measured to be 4.5 mb (calculation gave 5.1 mb but shifts the peak production to At). This gives a tentative indication that a rise in cross-section toward the region mass 200 may be real: this occurs in the calculation from fission competition to neutron emission only. As this low mass region is only reached via charged particle emission it is relatively little affected by fission as may be seen in Fig. 4 from the fictional spallation yield curve as calculated with fission disabled.

## 4 Final Comments

The inclusion of a fission treatment into HETC was motivated by practical needs. The treatment has been made as far as possible using either correlations from experiment and/or based on reasonable physical arguments. However, two particularly inadequate aspects remain: the need (i) to reduce the fission probability as obtained from the statistical model extrapolation and (ii) to by-pass fission in the case of charged particle emission. To what extent these are compensating for less-than-adequate treatments elsewhere in the overall particle-nucleus model is not known. That quite good agreement with measured fission cross-sections is obtained over a wide range of nuclei and excitation energies is some compensation.

**Acknowledgement**

The work on including fission into HETC was done in collaboration with Prof. Dr. J. Ranft of Leipzig University and while the author was a member of the Rutherford-Appleton Laboratory.

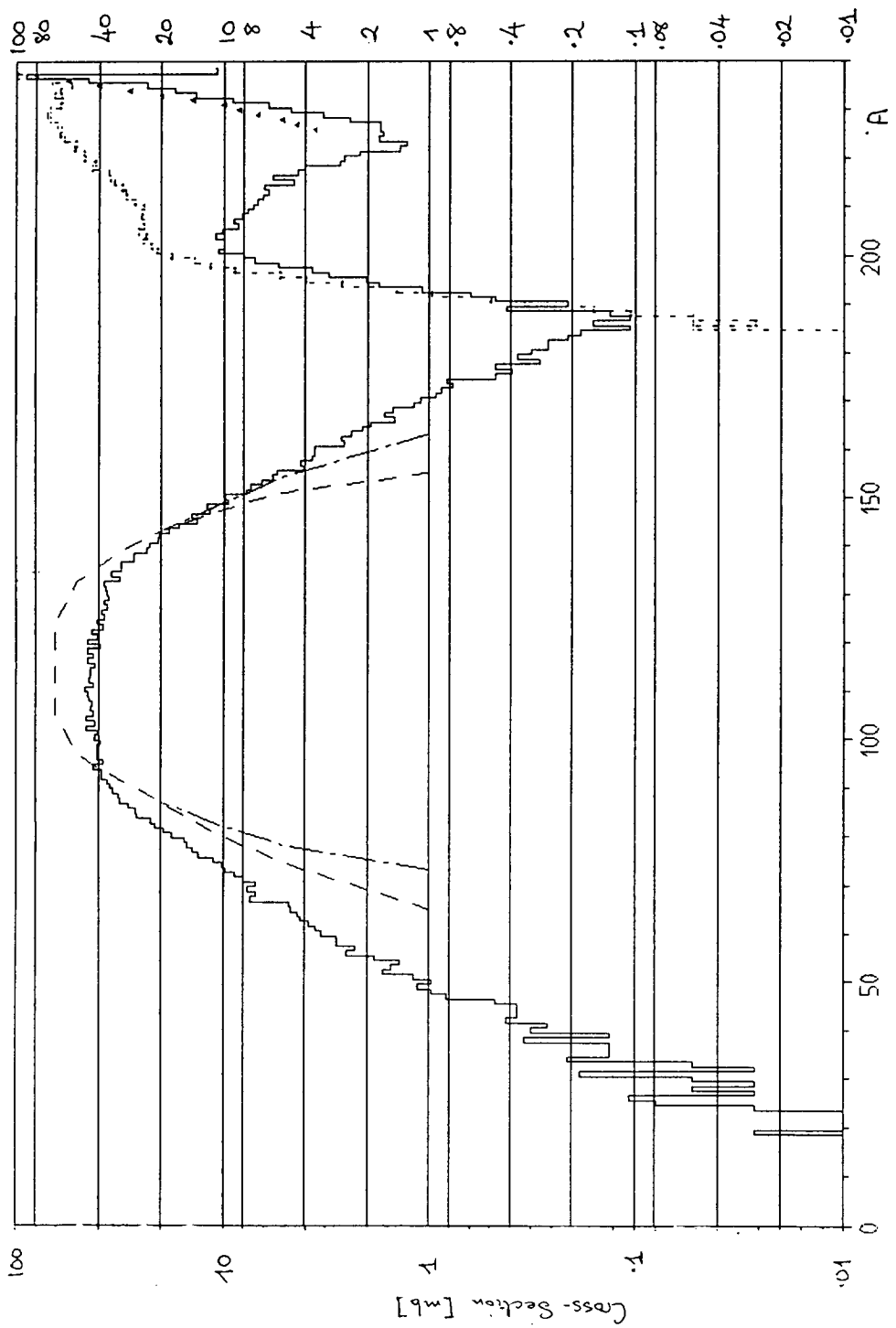


Figure 4: **The calculated mass distribution from bombardment of $^{238}U$ with 340 MeV protons. Measured values come from reference 53 for the fission products (dashed lines) and from reference 54 for the spallation products (triangles). For reference purposes the spallation product mass distribution with fission disabled is also shown.**

# References


1 K.C. Chandler and T.W. Armstrong Oak Ridge Report ORNL-4744 (1972)
2 RSIC computer code collection No. CCC-178
3 B. Boardman (Editor) Rutherford Lab. Report RL-82-006 (1982)
4 J.S. Fraser, R.E. Green, J.W. Hilborn, J.C.D. Milton, W.A. Gibson, E.E. Cross, A. Zucker Phys. Can. 21, 17 (1975)
5 F. Atchison Jül-Conf-34, paper II, 17 (1980)
6 F. Atchison Proc. Specialist' meeting on accelerator-based transmutation, PSI Villigen PSI-Proceedings 92-02, page 440 (1992)
7 I. Dostrovsky, Z. Frankel and P. Rabinowitz, Proc. 2nd UN Conf. Peaceful Uses of Atomic Energy, Geneva 1958 Paper P/1615, 15, 301 (1958)
8 M. Lindner and A. Turkevitch Phys. Rev 119, 1632 (1960)
9 R.L. Hahn and O.W Hermann, Oak Ridge National Lab. Report ORNL-TM-3179 (1971)
10 H.W. Bertini Phys. Rev 188, 174 (1969)
11 L.W. Dresner Oak Ridge Report ORNL-TM-196 (1962)
12 R. Serber Phys. Rev. 72, 1114 (1947)
13 R. Vandenbosch and J.R. Huizenger Proc. of 2nd Int. Conf. on Peaceful Uses of Atomic Energy, Geneva, paper P/688, Vol 15, page 284 (1958)
14 T. Sikkeland, J.E. Clarkson, N.H. Steiger-Shafir and V.E. Viola Phys. Rev. C3, 329 (1971)
15 H.R. Bowman, S.G. Thompson, J.C.D. Milton and W.J. Swiatecki Phys. Rev 126, 2120 (1962)
16 M. Dahlinger et al. Nucl. Phys. A376, 94 (1982)
17 V.F. Weisskopf Phys. Rev. 52, 295 (1937)
18 N. Bohr and J.A. Wheeler Phys. Rev. 56, 426 (1939)
19 B.B. Back, D. Hansen, H.C. Britt and J.D. Garrett Phys. Rev. C9, 1924 (1974)
20 T. Czyzewski, J. Dudck, M. Sowinski and J. Tya J. Phys G, 5, 1001 (1979)
21 D.S. Burnett, R.C. Gatti, F. Plasil, P.B. Price, W.J. Swiatecki and S.G. Thompson Phys. Rev. 134, B952 (1964)
22 B.B. Back, H.C. Britt, D. Hansen, B. Leroux and J.D. Garrett Phys. Rev. C10, 1948 (1974)
23 A. Gavron, H.C. Britt, E. Konescny, J. Weber and J.B. Wilhelmy Phys. Rev. C13, 2374 (1976)
24 J.R. Huizenga, R. Chaudhry and R. Vandenbosch Phys. Rev. 126, 1270 (1967)
25 G.M. Raisbeck and J.W. Cobble Phys. Rev. 153, 1270 (1967)
26 L.G. Moretto, S.G. Thompson, J. Routti and R.C. Gatti Phys. Lett. B36, 471 (1972)
27 V.E. Viola, Jr., and T. Sikkeland Phys. Rev. 128, 767 (1962)
28 K.J. Le Couteur Proc. Roy. Soc. A63, 259 (1950)
29 R. Vandenbosch and J.R. Huizenga Phys. Rev. 127, 212 (1962)
30 J.P. Unik, J.E. Grindler, L.E. Glendenin, K.F. Flynn, A. Gorski and R.K. Sjoblom Proc. 2nd Symp. on Physics & Chemistry of Fission, Rochester Vol II, page 19 (1973)
31 E.K. Hyde "The nuclear properties of the heavy elements", Vol III Prentice-Hall, New Jersey 1964
32 A. Smith, P. Fields, A. Friedman and R.S. Joblom Phys. Rev. 111, 1633 (1958)
33 J.C.D. Milton and J.S. Fraser Phys. Rev. 111, 877 (1958)
34 N.E. Stein and S.L. Whetstone Phys. Rev. 110, 476 (1958)
35 E.F. Neuzil and A.W. Fairhall Phys. Rev. 129, 2705 (1963)
36 G.T. Seaborg and R. Vandenbosch Phys. Rev. 110, 507 (1958)
37 A.H. Wapstra and G. Audi Nucl. Phys A432, 1 (1985)
38 J.H.E. Mattauch, W. Thiele and A.H. Wapstra Nucl. Phys. 67, 1 (1965)
39 A.G.W. Cameron Can. J. Phys. 35, 1021 (1957)
40 A.D. Taylor Rutherford Lab. Report RAL-84-120 (1984)
41 T.A. Broome Private communication (1989)
42 F. Atchison Rutherford Lab. Report RAL-81-006 (1981)
43 J.S. Gilmore, G.J. Russell, H. Robinson and R.E. Prael Nucl. Sci & Eng. 99, 41 (1988)
44 T.D. Thomas Phys. Rev. 116, 703 (1959)
45 G. Igo Phys. Rev. 115, 1665 (1959)
46 L.J. Colby, Jr., M.L. Shoaf and J.W. Cobble Phys. Rev. 121, 1415 (1961)
47 R. Vandenbosch, T.D. Thomas, S.E. Vandenbosch, R.A. Glass and G.T. Seaborg Phys. Rev. 111, 1358 (1958)
48 J. Wing, W.J. Ramler, A.L. Harkness and J.R. Huizenga Phys. Rev. 114, 163 (1959)
49 R.A. Glass, R.J. Carr, J.W. Cobble, G.T. Seaborg Phys. Rev. 104, 434 (1956)
50 B.M. Foreman, Jr. W.M. Gibson, R.A. Glass and G.T. Seaborg Phys. Rev. 116, 382 (1959)
51 R. Vandenbosch and G.T. Seaborg Phys. Rev. 110, 507 (1958)
52 A. Chetham-Strode, Jr., G.R. Choppin and B.G. Harvey Phys. Rev. 102, 747 (1956)
53 P.C. Stevenson, H.G. Hicks, W.E. Nevik and D.R. Nethaway Phys. Rev. 111, 886 (1958)
54 M. Lindner and R.N. Osborne Phys. Rev. 103, 378 (1956)
55 H.M. Steiner and J.A. Jungerman Phys. Rev. 101, 807 (1956)
56 V.A. Kon'shin, E.S. Matusevich and V.I. Regushevskii Sov. J. Nucl. Phys. 2, 489 (1966)
57 L.G. Jodra and N. Sugarman Phys. Rev. 99, 1470 (1955)
58 P. Kruger and N. Sugarman Phys. Rev. 99, 1459 (1955)

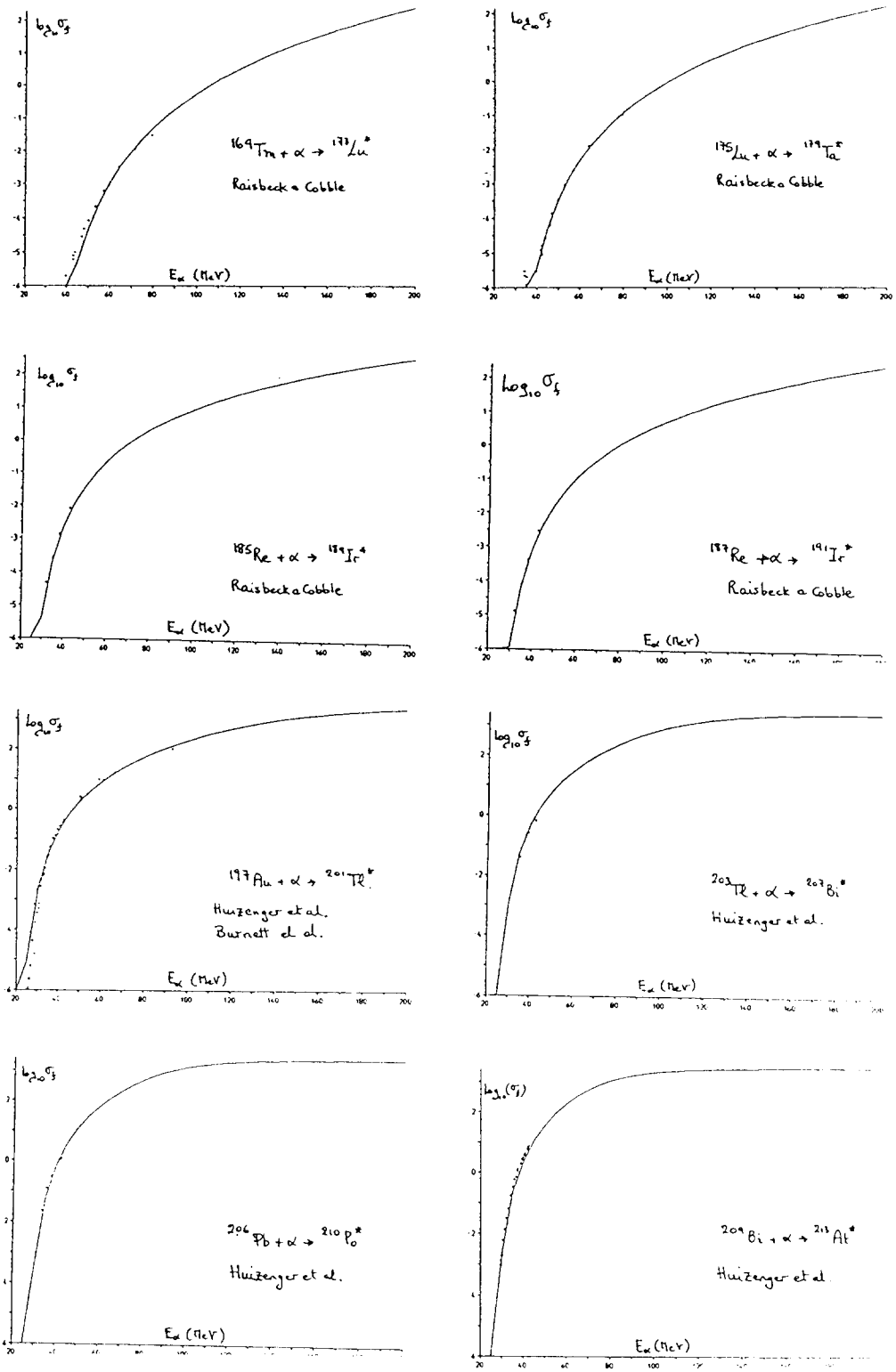


Figure 19: A selection of $\alpha$-particle induced fission cross-sections for elements up to Bi. The dots are experimental data and come from Raisbeck & Cobble [88], Huizenger et al. [89] and Burnett et al. [90]. The lines are the results of calculation.

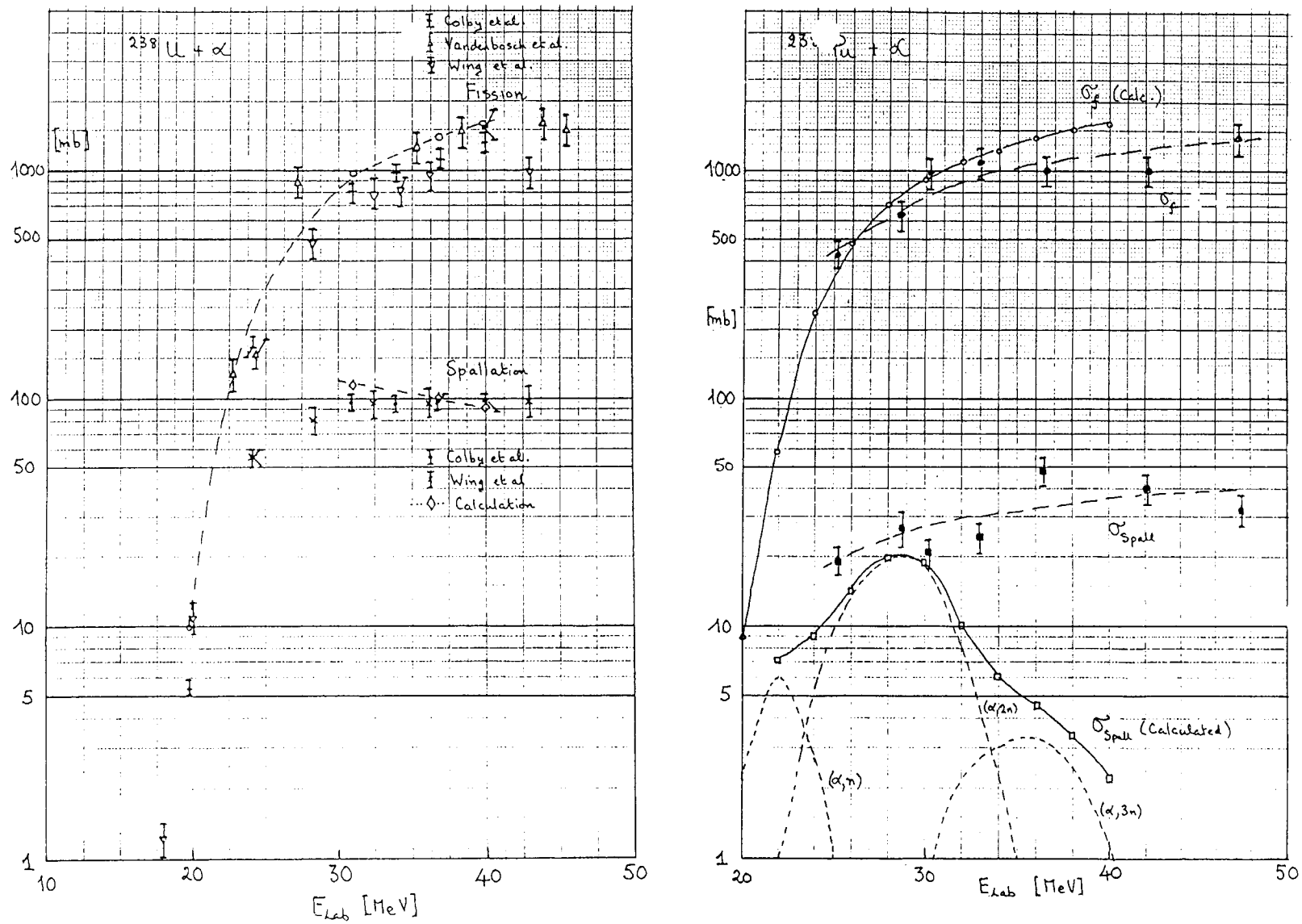


Figure 20: Calculated and measured α-particle induced cross-sections for fission and spallation of $^{238}U$ (results from references 93, 95, 94) and $^{238}Pu$ (results from reference 97).

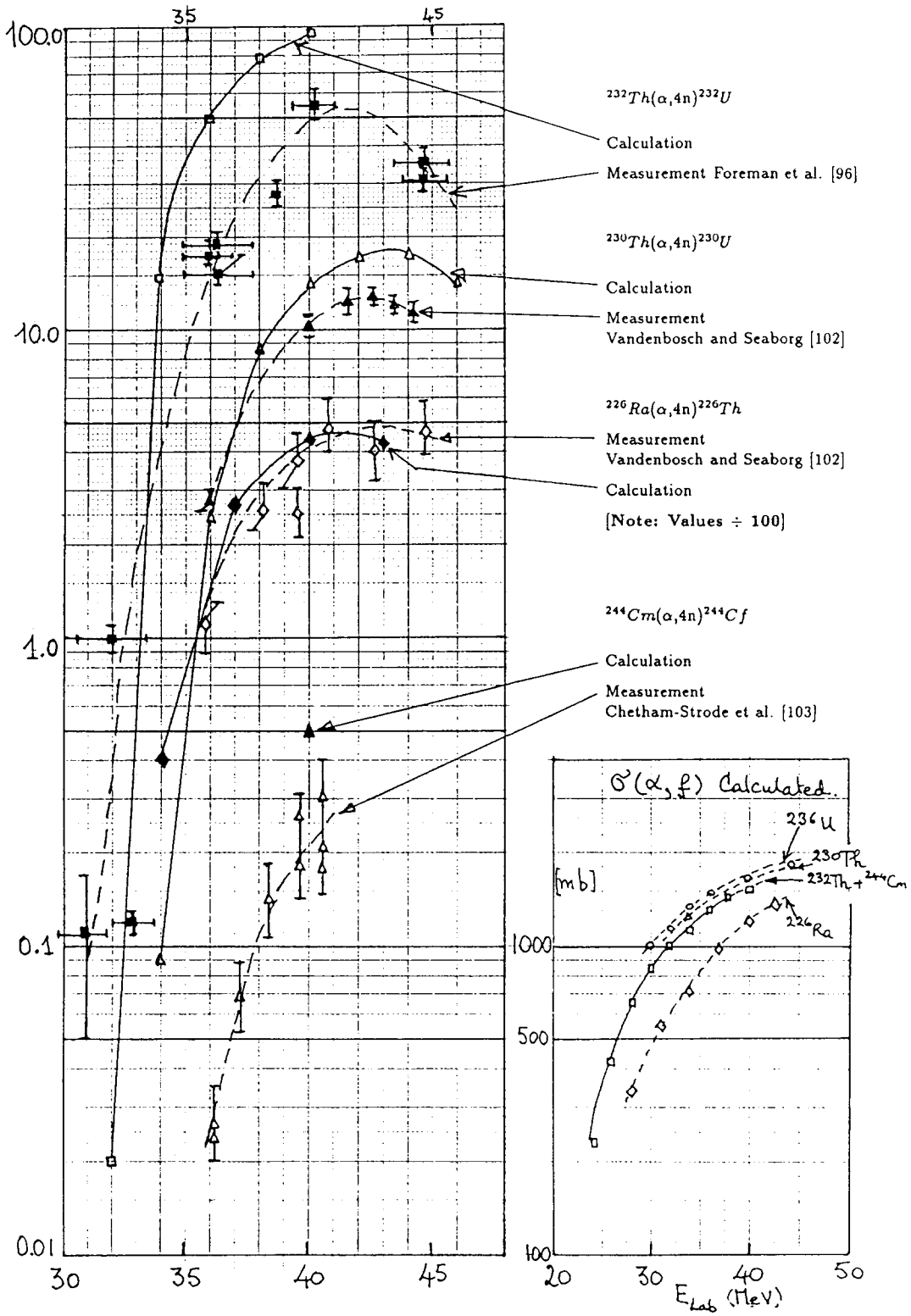


Figure 21: Calculated and measured (α,4n) cross-sections for $^{226}Ra$ [102], $^{230}Th$ [102], $^{232}Th$ [96] and $^{244}Cm$ [103]. For reference, the calculated fission cross-sections are included as an insert.

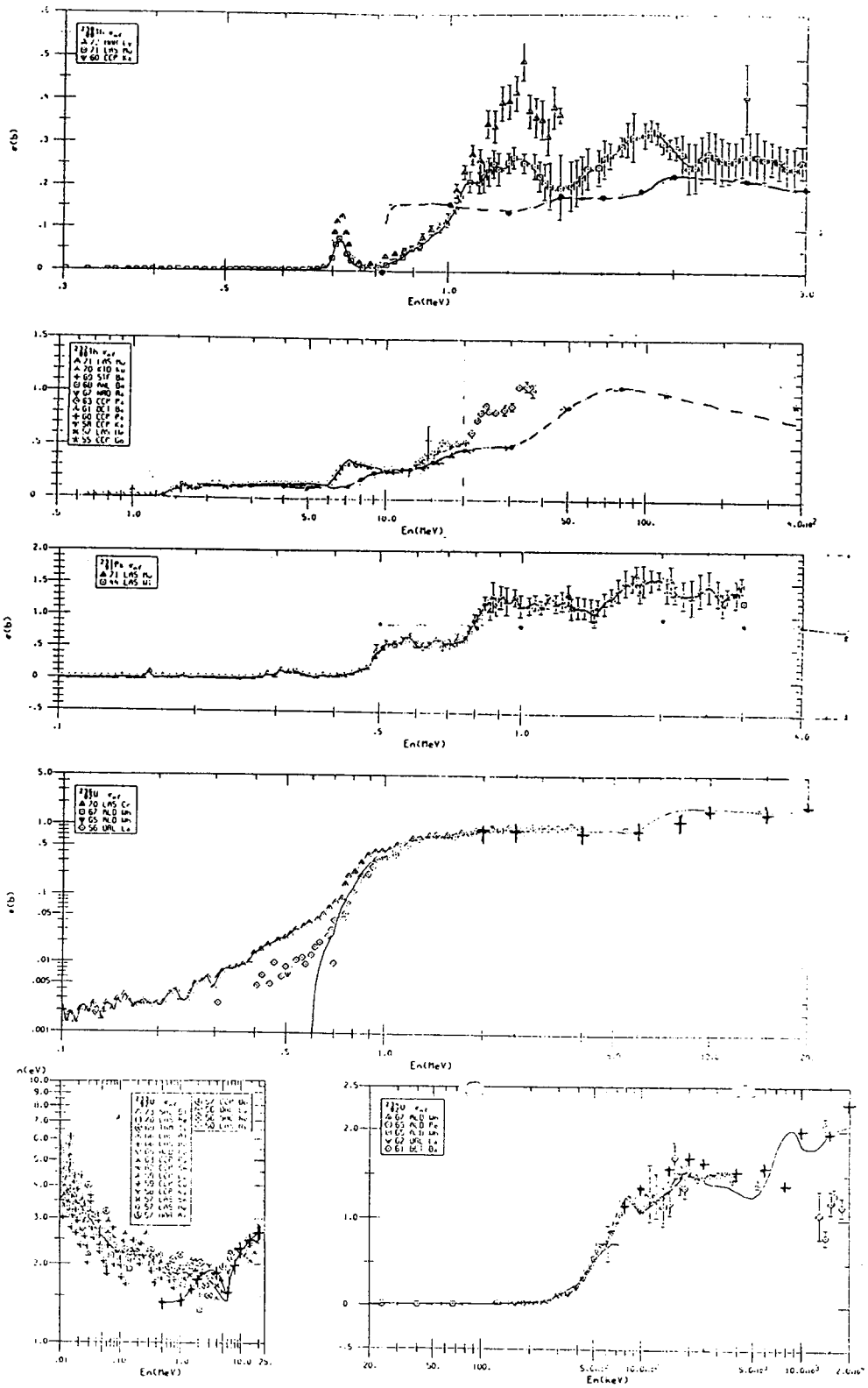

Figure 22: Fast neutron induced fission cross-sections.

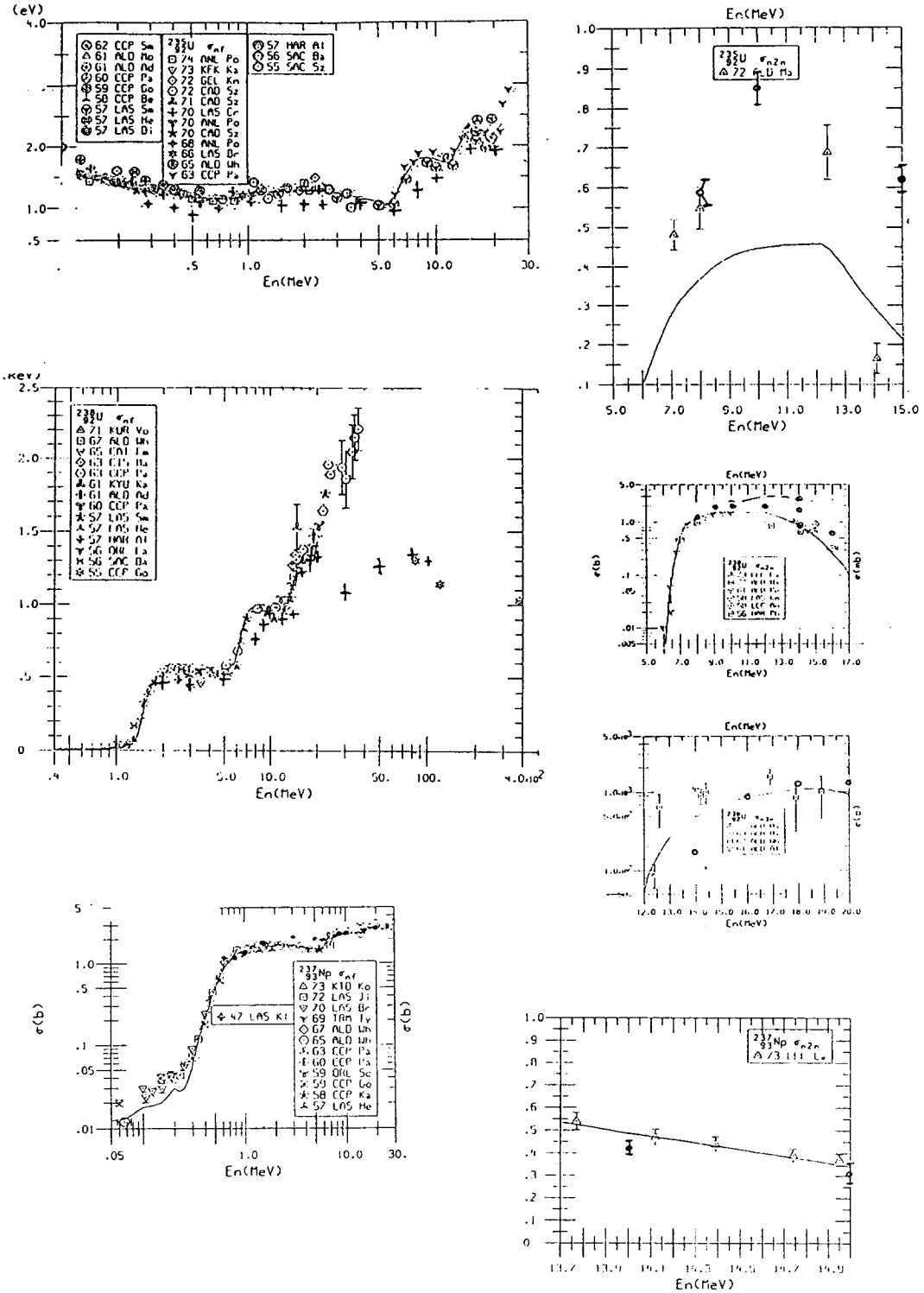


Figure 23: Fast neutron induced fission cross-sections.

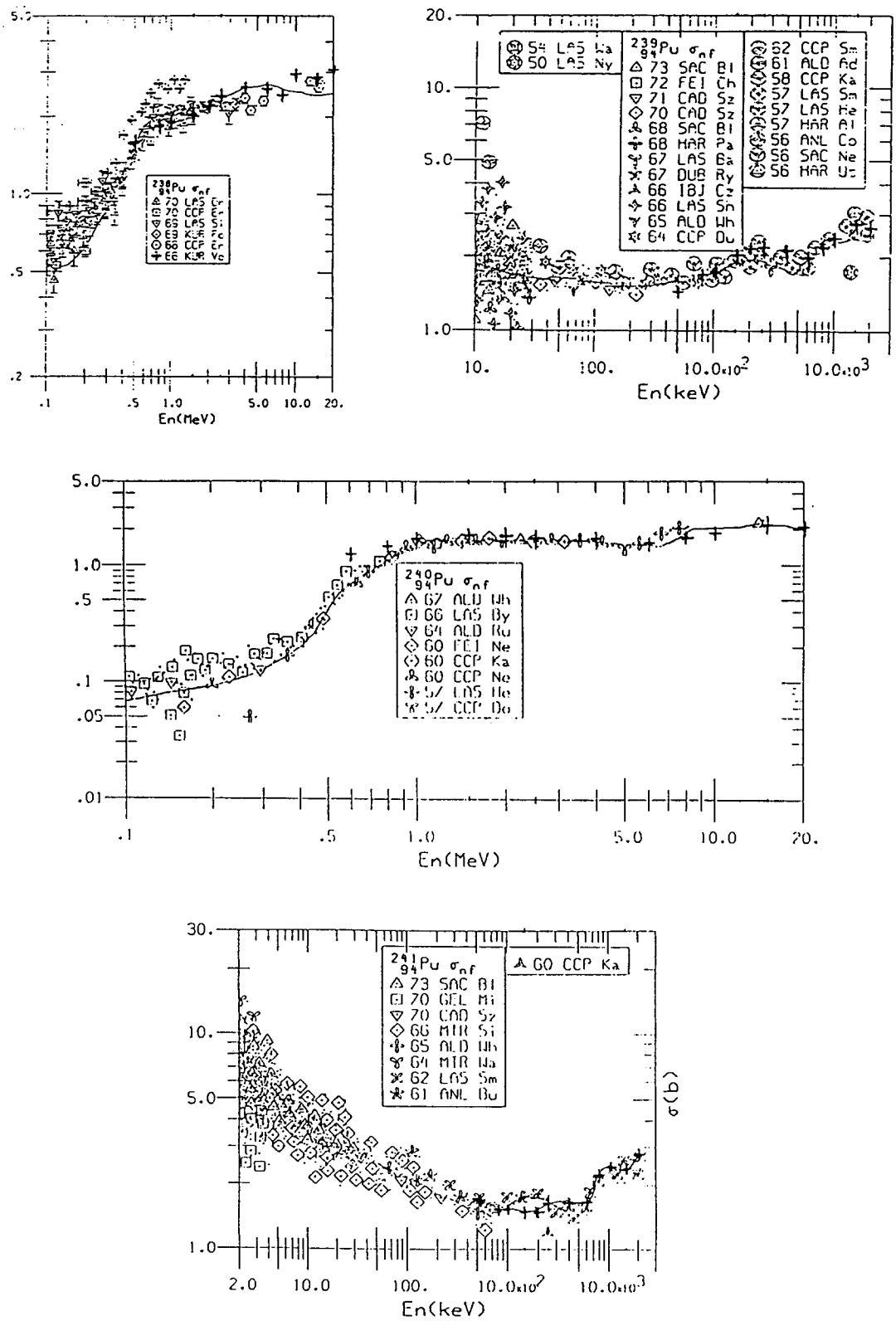


Figure 24: Fast neutron induced fission cross-sections.

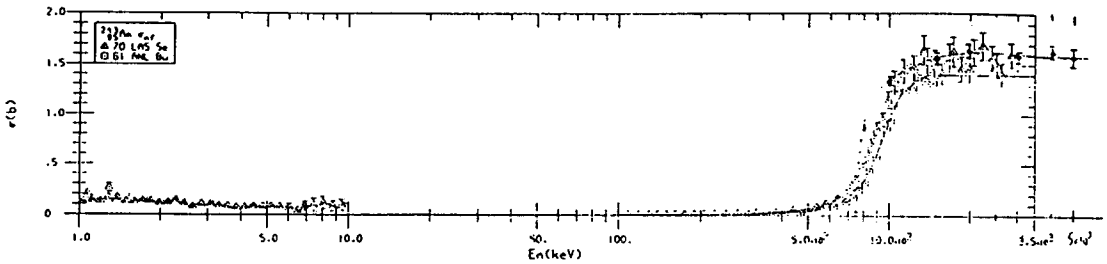


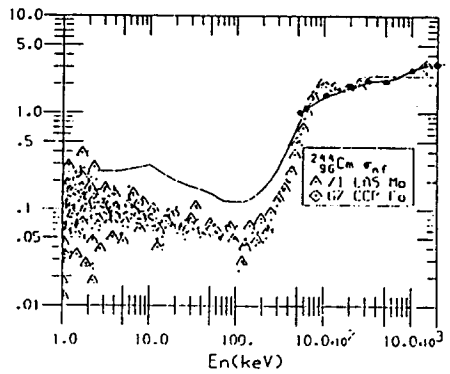


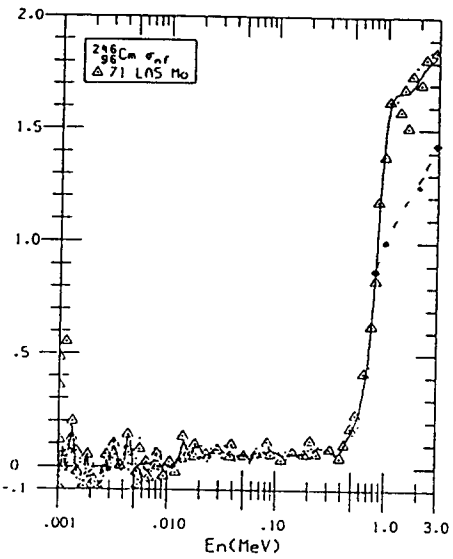


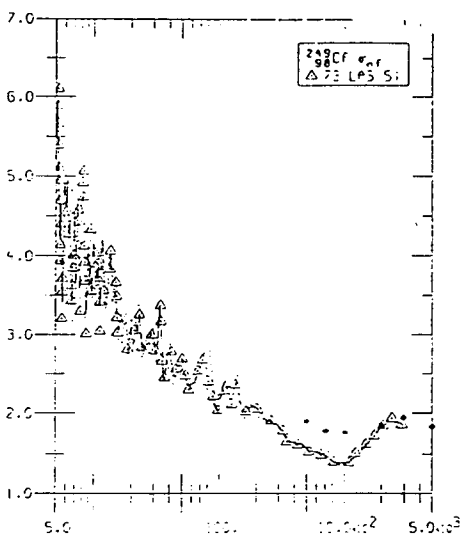

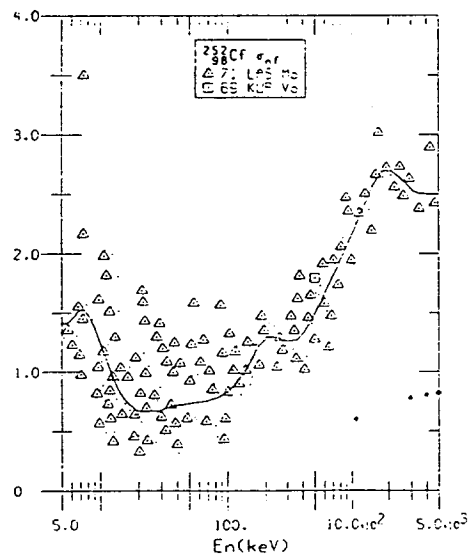


Figure 25: Fast neutron induced fission cross-sections.

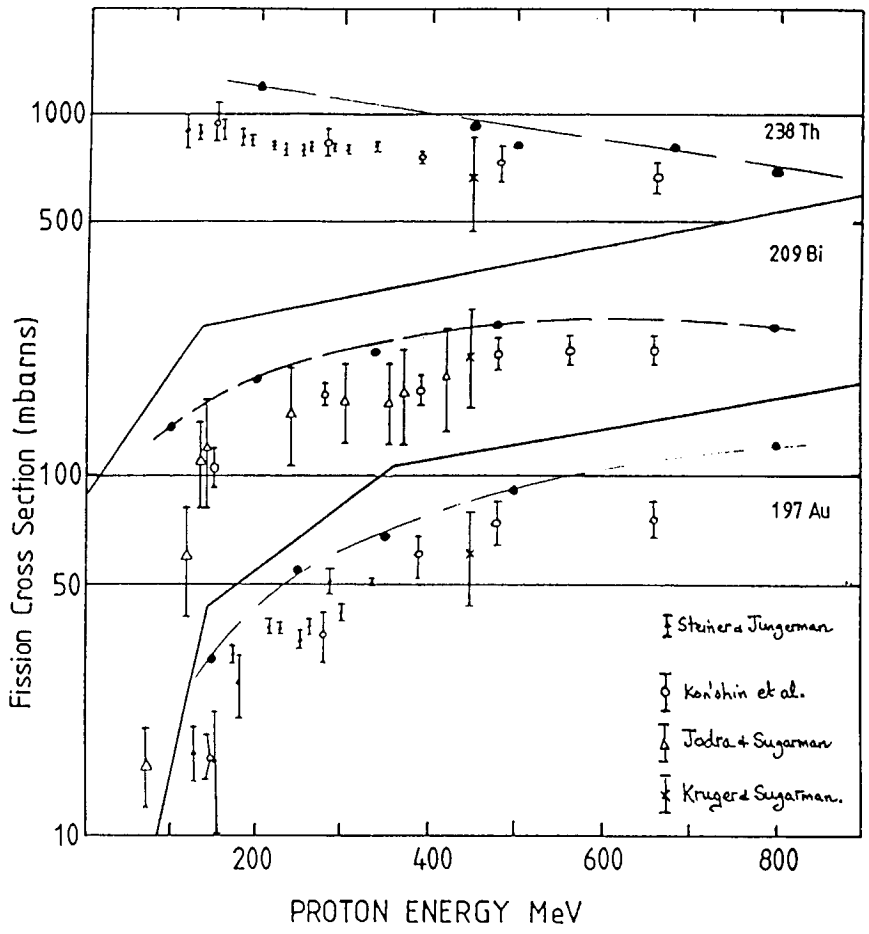


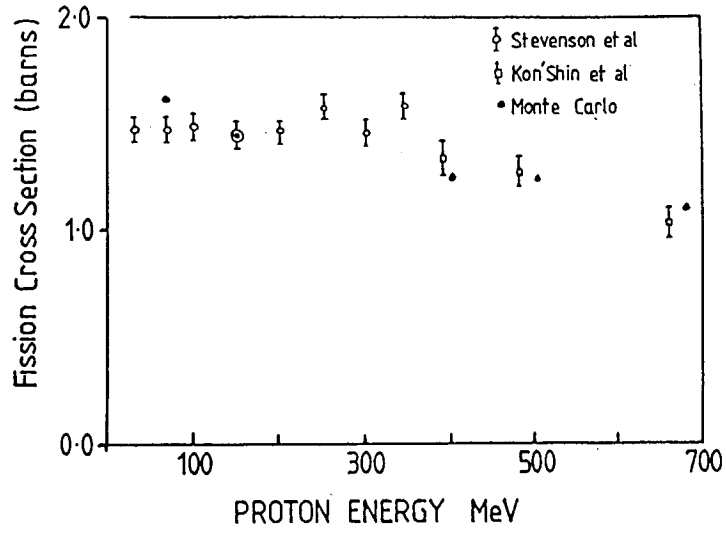


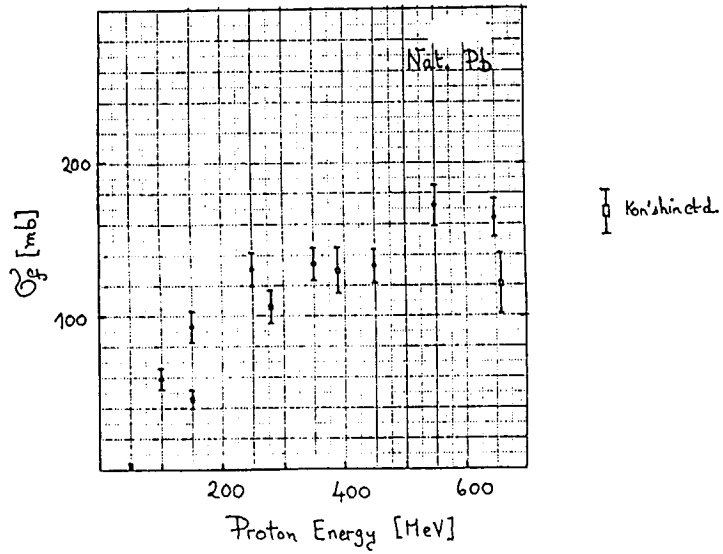


Figure 26: High-energy proton induced fission cross-sections.